TUDelft

Delft University of Technology

Critical Short Circuit Ratio of an EV Charging System

Wang, L.; Qin, Z.; Xiao, J.; Bauer, P.

Citation (APA)
Wang, L., Qin, Z., Xiao, J., & Bauer, P. (2023). Critical Short Circuit Ratio of an EV Charging System. In *2023 25th European Conference on Power Electronics and Applications, EPE 2023 ECCE Europe* (2023 25th European Conference on Power Electronics and Applications, EPE 2023 ECCE Europe). IEEE. https://doi.org/10.23919/EPE23ECCEEurope58414.2023.10264322

Important note
To cite this publication, please use the final published version (if applicable).
Please check the document version above.

Critical Short Circuit Ratio of an EV Charging System

Lu Wang, Zian Qin, Junjie Xiao, Pavol Bauer

Department of Electrical Sustainable Energy

Delft University of Technology

Mekelweg 4

Delft, The Netherlands

E-Mail: l.wang-11@tudelft.nl, z.qin-2@tudelft.nl, j.xiao-2@tudelft.nl, p.bauer@tudelft.nl

Index Terms—**Grid-connected converter, Power converters for EV, Power system stability, Voltage Source Converters (VSCs).**

Abstract—**The critical short circuit ratio (CSCR), as an important metric for grid stability evaluation, is not clearly defined in the literature. Aimed at clarifying the misunderstandings, the paper compares the different CSCR definitions. Moreover, CSCR reduction-oriented design is studied for electric vehicle chargers. Simulations verify the analysis.**

I. INTRODUCTION

Amid the transition to more electrified transportation systems, recent years witnessed a world-widely increase in the market share of electric vehicles (EVs). Consequently, to fulfill the charging demand, enormous EV chargers are or will be connected to power grids [1], [2]. Nevertheless, connecting EV chargers, which are power-electronic-based loads, to a grid may threaten the grid's stability. Previous studies [3]–[7] reveal that if the grid strength, which can be quantified by the short circuit ratio (SCR), is low at the point of common coupling (PCC), a grid-converter system, including the grid-converter system, may be unstable. Therefore, defining a critical SCR (CSCR), which is the lowest SCR to keep the grid's stability, is convenient for stability evaluation.

However, the definition of the CSCR is different among the works in the literature. In [4], the CSCR is defined from the voltage stability perspective. According to the power flow analysis, under a fixed power factor, the active power absorbed at a certain PCC in the power system network has a maximum, which is determined by the SCR and the grid impedance ratio (GIR) at the PCC [8]. If the load power at the PCC exceeds the maximum, the grid voltages at the PCC collapse, and thereby instability happens. Conversely, for a given load whose maximum power is fixed, the lowest SCR to keep the voltage stability can be derived under a given GIR. Thus, the derived lowest SCR is referred to as the CSCR.

Later on, the small-signal stability of power-electronic-based systems is studied [3], [5]–[7]. Different from voltage instability, small-signal instability is caused by the underdamped resonance between the grid and the grid-tied converter, i.e., inverters or rectifiers. Based on the modeling of grid-tied converters' input impedance in the frequency domain, the general Nyquist criterion (GNC) [9] can be applied to evaluate the small-signal stability of a grid-converter system with a simplified impedance-based model [3]. More studies [10] reveal that such small-signal instability may happen when the SCR is low. Consequently, a CSCR indicating the lowest SCR to keep system stability can be defined [11].

Apparently, the two definitions of the CSCR are different from each other. For clarity, the CSCR defined from the voltage stability perspective is referred to as $CSCR_v$ while the other one is named as $CSCR_s$. However, for a given system, there should be only one CSCR which stands for the lowest SCR to maintain system stability. Thus, the bigger one between the $CSCR_v$ and the $CSCR_s$ is the real CSCR. Nevertheless, which one between the two is bigger is not consistent from case to case. Consequently, both of the two should be calculated for each case. However, calculating the $CSCR_v$ and

the CSCR_s are complicated [11], which brings more challenges to obtaining the CSCR in practice.

Aimed at clarifying the misunderstandings, the paper compares the differences between the CSCR_v and the CSCR_s. Both of them need to be calculated to obtain the CSCR of a grid-converter system including the EV charging system. Further, to approximate the CSCR easily in practice, the simplified calculation method for an EV charging system, whose power factor (PF) is high, is presented. Besides, to prepare for the weak grid connections coming sooner or later, the design of an EV charger to enhance the robustness of the charging system against the grid strength weakening is studied. Briefly, the CSCR_v can be reduced by increasing the charger's reactive power injection. As for the CSCR_s, it is mainly determined by the control of the charger's grid-tied converter. Therefore, the impact of the control loops, namely the current loop (CL) and the voltage loop (VL), on the charger's input impedance and eventually the CSCR_s of the charging system is studied. As a result, the design guidelines to reduce the CSCR_s are given, which is beneficial for reducing the CSCR of the charging system.

This paper is organized as follows. Section II reviews the voltage stability criterion and presents the simplified calculation of the CSCR_v for an EV charging system. Section III shows the small-signal criterion and its simplification for an EV charging system, which ends up with the simplified calculation of the CSCR_s. A comparison study between the CSCR_v and the CSCR_s is given in Section IV. Moreover, design guidelines to reduce the CSCR are summarized. In Section V, conclusions are drawn.

II. VOLTAGE STABILITY ANALYSIS AND THE CSCR_v

A. Maximum power transfer theorem

The simplified model of a three-phase charging system for voltage stability analysis is illustrated in Fig. 1, where the grid is simplified as a voltage source $E_g \; \underline{/0}$ and a grid impedance Z_g. For simplicity, the phase of the grid voltage phasor is assumed zero. The PCC voltage is $U \; \underline{/\theta}$ while the apparent power absorbed at the PCC is S.

The complex grid current can be derived, which is

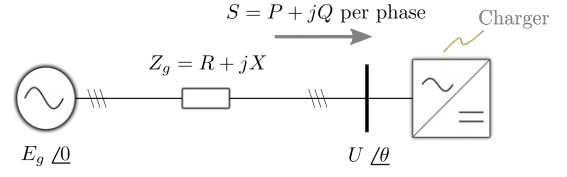$$I = \frac{E_g - U\cos(\theta) - jU\sin(\theta)}{R + jX}. \tag{1}$$

Fig. 1. Simplified model of a three-phase charging system for voltage stability analysis

Since $S = UI^*$, the active power P and the reactive power Q absorbed at the PCC are

$$\begin{cases} P = \dfrac{UE_g R\cos(\theta) - UE_g X\sin(\theta) - U^2 R}{R^2 + X^2} \\ Q = \dfrac{UE_g R\sin(\theta) + UE_g X\cos(\theta) - U^2 X}{R^2 + X^2} \end{cases} \tag{2}$$

Eliminating θ from (2) gives

$$U^4 + (2(PR+QX) - E_g^2)U^2 + (R^2+X^2)(P^2+Q^2) = 0. \tag{3}$$

The condition for (3), which is a second order equation of U^2, to have at least one solution is

$$(2(PR+QX) - E_g^2)^2 - 4(R^2+X^2)(P^2+Q^2) \geq 0, \tag{4}$$

which can be simplified as

$$1 - 4\frac{PR+QX}{E_g^2} - 4\left(\frac{PX-QR}{E_g^2}\right)^2 \geq 0. \tag{5}$$

The left hand side of (5) can be rewritten as a second order function with respect to P, which is given by

$$f(P) = c + \frac{b^2}{4a} - a\left(P + \frac{b}{2a}\right)^2, \tag{6}$$

where

$$\begin{cases} a = 4X^2 \\ b = 4E_g^2 R - 8QRX \\ c = E_g^4 - 4Q^2 R^2 - 4E_g^2 QX \end{cases} \tag{7}$$

Clearly, when $f(P) = 0$, P reaches the maximum. When $f(P) = 0$, the positive solution of P corresponds to the maximum load while the negative one is the maximum generation.

B. Calculation of the CSCR_v

For the three-phase system illustrated in Fig. 1, the SCR at the PCC can be calculated as

$$\text{SCR} = \frac{S_{SC}}{S_L} = \frac{E_g^2}{|Z_g||S|} = \frac{E_g^2}{\sqrt{(P^2+Q^2)(R^2+X^2)}}, \tag{8}$$

where S_{SC} is the short circuit capacity and S_L is the load capacity of one phase.

Substituting (8) into (5) gives

$$1 - 2\alpha \frac{2}{|S| \cdot \text{SCR}} - \beta^2 (\frac{2}{|S| \cdot \text{SCR}})^2 \geq 0, \qquad (9)$$

where

$$\begin{cases} \alpha = \dfrac{P + Q(X/R)}{\sqrt{1 + (X/R)^2}} \\[3mm] \beta = \dfrac{P(X/R) - Q}{\sqrt{1 + (X/R)^2}} \end{cases} \qquad (10)$$

(9) can be rewritten as

$$\frac{\beta^2 + \alpha^2}{\beta^4} \geq (\frac{\alpha}{\beta^2} + \frac{2}{|S| \cdot \text{SCR}})^2. \qquad (11)$$

Since SCR is positive, (11) can be simplified as

$$\begin{cases} 0 < \dfrac{2}{|S|\text{SCR}} \leq \dfrac{\sqrt{\alpha^2 + \beta^2} - \alpha}{\beta^2} & (\alpha \geq 0) \\[3mm] 0 < \dfrac{2}{|S|\text{SCR}} \leq -\dfrac{\alpha}{\beta^2} & (\alpha < 0) \end{cases} \qquad (12)$$

Therefore, for a load whose capacity $|S|$ and PF are fixed, the condition for (3) to have at least one solution is given by

$$\begin{cases} \text{SCR} \geq \dfrac{2}{|S|} \dfrac{\beta^2}{\sqrt{\alpha^2 + \beta^2} - \alpha} & (\alpha \geq 0) \\[3mm] \text{SCR} \geq -\dfrac{2}{|S|} \dfrac{\beta^2}{\alpha} & (\alpha < 0) \end{cases} \qquad (13)$$

(13) indicates that for a grid-tied converter, the CSCR_v when it operates in the inverter mode, i.e., $\alpha < 0$, is different from the one in the rectifier mode, i.e., $\alpha \geq 0$.

Finally, by substituting (10) into (13), the expression of the CSCR_v in the rectifier mode can be obtained as

$$\text{CSCR}_{v1} = \frac{2}{|S|} \frac{(P\frac{X}{R} - Q)^2}{(|S|\sqrt{1 + (\frac{X}{R})^2} - Q\frac{X}{R} - P)\sqrt{1 + (\frac{X}{R})^2}}. \qquad (14)$$

The CSCR_v in the inverter mode is given by

$$\text{CSCR}_{v2} = -\frac{2}{|S|} \frac{(P\frac{X}{R} - Q)^2}{\sqrt{1 + (\frac{X}{R})^2}(Q\frac{X}{R} + P)}. \qquad (15)$$

Only the rectifier mode is considered for simplicity since the paper focuses on the CSCR of charging systems. As seen, the GIR, i.e., X/R has an influence on the CSCR. In order to further simplify (14), two scenarios are considered.

1) GIR tends to zero

$$\text{CSCR}_v = \frac{2}{|S|} \frac{Q^2}{|S| - P}. \qquad (16)$$

The range of the $CSCR_v$ is [0,2] because the range of the Q is $[0, |S|]$.

2) GIR tends to infinite

$$\text{CSCR}_v = \frac{2}{|S|} \frac{P^2}{|S| - Q}. \qquad (17)$$

Similarly, it can be seen $CSCR_v \in [0,2]$.

Generally, the chargers' PFs are unity. Therefore, the CSCR_v is higher if the GIR is larger. The worst case is the situation when the GIR is infinite, which leads to the maximum CSCR_v value, i.e., 2. This worst case is considered to ensure the stability of the charging system in different grid conditions.

C. Verification of the CSCR$_v$

A charging system illustrated in Fig. 1 is simulated to verify the derived CSCR_v. The charger is simplified as a three-phase current load whose active power is fixed at 30 kW and reactive power is zero. In this way, the control of the charger is neglected, and thereby the small-signal instability will not happen. The grid impedance is assumed purely inductive as the worst case. The inductance of the grid impedance gradually increases to decrease the SCR to the CSCR_v.
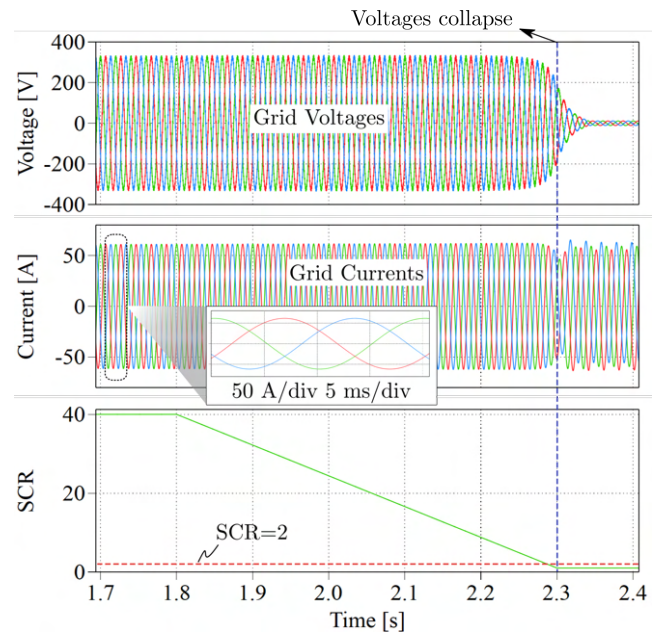

Fig. 2. Simulation of the CSCR$_v$ of a 30-kW charging system

Fig. 2 depicts the simulation results. Clearly, when the SCR reaches 2, the grid voltages start to collapse,

evincing the system is unstable. As a result, the charger cannot draw power from the power grid anymore.

III. SMALL-SIGNAL STABILITY ANALYSIS AND THE CSCR$_s$

A. Impedance based stability analysis

The small-signal stability of a three-phase charging system can be evaluated with the impedance-based analysis [3], [12], [13]. The analysis is based on the model depicted in Fig. 3. Such a model can be established in either the sequence domain or the synchronized dq-frame.
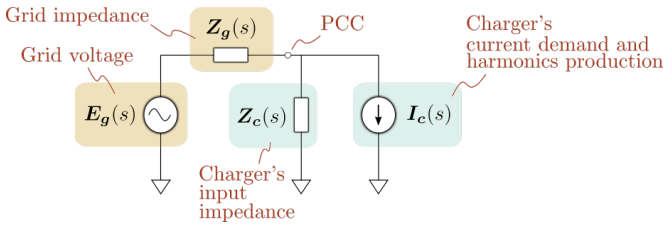

Fig. 3. Impedance model of a three-phase charging system

The input impedance of an EV charger is mainly determined by the grid-tied rectifier of the EV charger. More specifically, the power filter and the control of the grid-tied rectifier have the dominant influence on the input impedance, which is similar to the other grid-tied converters [14]. Typical designs of EV chargers' rectifiers are elaborated in [15], [16]. As an example, the typical circuit and control system of an EV charger's rectifier shown in Fig. 4 is considered to demonstrate the small-signal stability criterion. The control system consists of a phase lock loop (PLL), alternating current control (ACC), and direct voltage control (DVC).
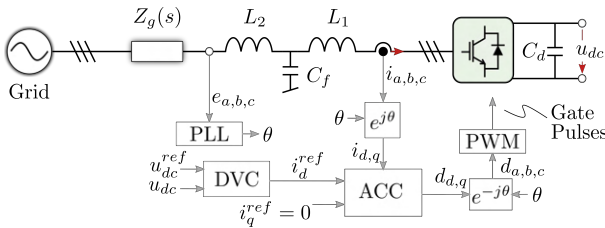

Fig. 4. Typical circuit and control system of an EV charger's rectifier

Such a rectifier is also known as the active front end (AFE) converter whose input impedance modeling is well studied in [17]. Accordingly, the charger's input impedance can be extracted analytically, which is obtained as

$$\boldsymbol{Z_c}(s) = \begin{bmatrix} Z_{dd}(s) & Z_{dq}(s) \\ Z_{qd}(s) & Z_{qq}(s) \end{bmatrix}. \quad (18)$$

The model given by (18) is in the synchronized dq-frame. The grid impedance in the same dq-frame is given by

$$\boldsymbol{Z_g}(s) = \begin{bmatrix} Z_{g,dd}(s) & Z_{g,dq} \\ Z_{g,qd} & Z_{g,qq}(s) \end{bmatrix} = \begin{bmatrix} L_g s & -\omega_1 L_g \\ \omega_1 L_g & L_g s \end{bmatrix}. \quad (19)$$

Based on the extracted charger's input impedance, the grid impedance, and the model in Fig. 3, the small-signal stability can be evaluated by studying the eigenvalues of the characteristic equation given by

$$det(\boldsymbol{I} + \boldsymbol{Z_g}(s)\boldsymbol{Y_c}(s)) = 0, \quad (20)$$

where I is a two-by-two unit matrix. If the eigenvalues of (20) are all in the left half on the complex plane, the system is stable otherwise not. Alternatively, the system's stability can be analyzed with the return-ratio matrix

$$\boldsymbol{L} = \boldsymbol{Z_g}(s)\boldsymbol{Y_c}(s). \quad (21)$$

Based on the eigen-loci of $\boldsymbol{L}$, the GNC [9] can be applied for the stability evaluation. As an example, the stability of a charging system, whose specifications are shown in Table I, is studied.

TABLE I
SPECIFICATIONS OF THE CHARGING SYSTEM UNDER SUTDY

Param.	Description	Value
E_g	Grid voltage	230 Vrms
f_1	Grid frequency	50 Hz
L_1	LCL-filter converter side inductance	300 μH
L_2	LCL-filter grid side inductance	300 μH
C_f	LCL-filter capacitance	10 μF
C_d	AFE output capacitance	3 mF
$f_{c,PLL}$	PLL cutoff frequency	10 Hz
δ_{PLL}	PLL damping ratio	2
$f_{c,CL}$	CL cutoff frequency	800 Hz
δ_{CL}	CL damping ratio	1
$f_{c,VL}$	VL cutoff frequency	30 Hz
$\delta_{c,VL}$	VL damping ratio	1

The eigen-loci of the $\boldsymbol{L}$ of a grid-charger system are shown in Fig. 5. As seen, when the SCR is as small as 8.4, the eigen-loci do not encircle the critical point -1+j0, indicating that the grid-charger system is stable. However, when the SCR decreases to 2.8, the eigen-loci encircle the -1+j0 point twice in the clockwise direction, indicating the characteristic equation has two eigenvalues in the right-half plane, and thereby the system is unstable.

Fig. 5 clearly illustrates that when the SCR decreases, the area encircled by the eigen-loci expands. When the SCR equals CSCR$_s$, at least one of the eigen-loci cross the -1+j0 point, which is a boundary scenario. However,
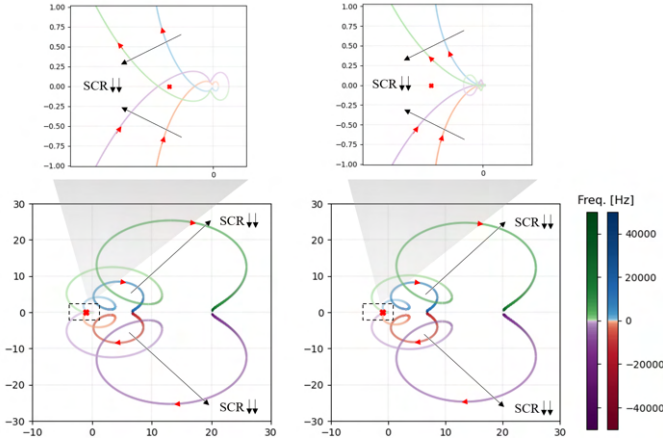
Fig. 5. Eigen-loci the $\boldsymbol{L}$ of the grid-charger system with different SCR. The red-blue curves are the eigen-loci when SCR=8.4 whereas the purple-green curves are the eigen-loci when SCR=2.8. Clearly, when the SCR is small, the grid-charger system is unstable because the -1+j0 point is encircled by the eigen-locus shown on the left-hand side.

applying GNC to find the CSCR_s is apparently tricky because it requires many iterations to approximate the CSCR_s. Thus, a simplified approach is needed.

B. Simplified derivation of the $CSCR_s$

The simplification of the GNC for high PF three-phase rectifiers is studied in [18]. Accordingly, for a grid-tied converter with a high PF, e.g. an EV charger, the coupling impedance $Z_{dq}(s)$ and $Z_{qd}(s)$ is much smaller than the diagonal impedance $Z_{dd}(s)$ and $Z_{qq}(s)$. Consequently, the stability of the charging system, which is a multiple-input multiple-output (MIMO) system, can be analyzed with the two single-input single-output (SISO) systems in the d-axis and the q-axis, respectively. Therefore, bode plots of the $Z_{dd}(s)$ and the $Z_{qq}(s)$, instead of the eigen-loci of the return-ratio matrix $\boldsymbol{L}$, can be used for the stability analysis. For clarity, the simplified stability criterion is illustrated in Fig. 6. As seen from Fig. 6a, the phase of the $Z_{dd}(s)$ is between $-90°$ and $90°$ below 100 Hz. Such indicates the real part of the $Z_{dd}(s)$ is negative, which is impossible for a passive component, e.g. a resistor. Thus, the region below 100 Hz is called the non-passive region [7]. When SCR=8.4, the resonant frequency f_{rd1} locates outside the non-passive region, indicating that the grid-charger system is stable. However, when the SCR decreases to 2.8, the resonant frequency decreases to f_{rd3} located inside the non-passive region, thereby making the system unstable because of the underdamped resonance induced by the negative resistance. When the resonant frequency is located at the non-passive region's maximum frequency,

the corresponding SCR is the CSCR_s. Accordingly, the CSCR_s equals 3.74 in this case.
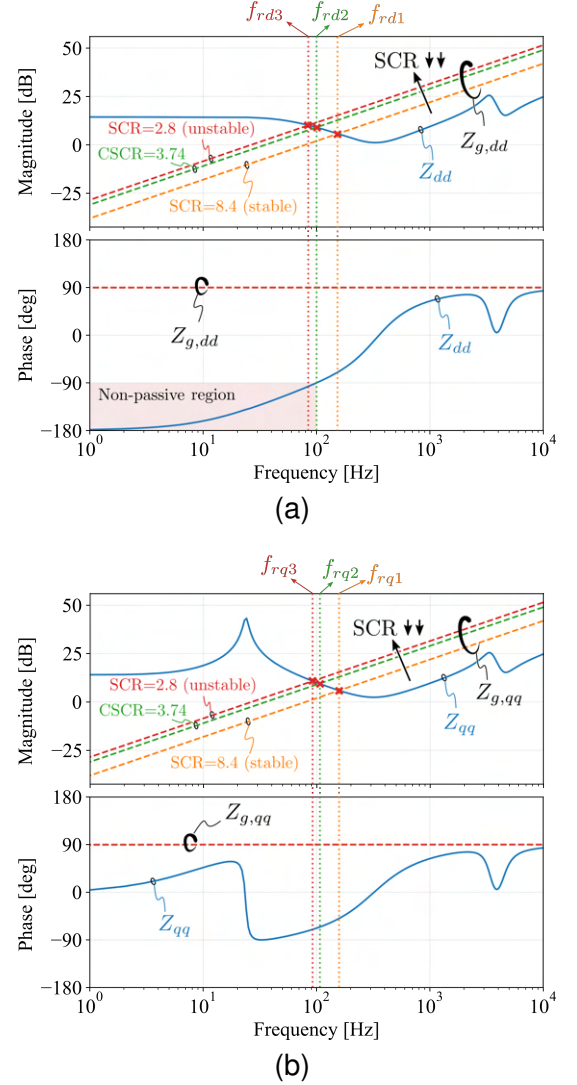

(a)

(b)

Fig. 6. Bode plots of the (a) $Z_{dd}(s)$ and (b) $Z_{qq}(s)$ and the grid impedance with different SCR. Instability happens when the resonant frequency of the grid-charger system locates in the non-passive frequency range.

C. Verification of the $CSCR_s$

The stability of the charging system specified by Table I is simulated. Fig. 7 shows the simulation results evincing that the system is stable when the SCR is high but is unstable when the SCR is just below the derived CSCR_s, which is higher than the CSCR_v. Besides, it is noted that instability does not happen immediately when the SCR decreases to just below the CSCR_s. Instead, the charging system gradually becomes unstable, proving that it is a small-signal instability issue that happens at this steady state.
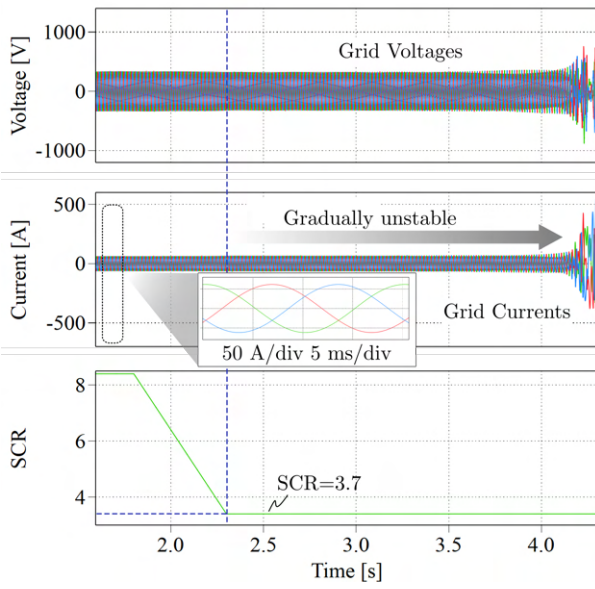
Fig. 7. Simulation shows the charging system is unstable when the SCR is just below the derived $CSCR_s$

IV. CRITICAL SHORT CIRCUIT RATIO REDUCTION ORIENTED DESIGN

The power grid tends to get weaker with the growing renewable energy generation. Requirements for weak grid connection compatibility are already seen for distributed energy resources [19]. The same requirement for EV chargers is expected to come sooner or later. Therefore, the method to reduce a charger's CSCR for weak grid connections is presented in this section.

Previous analysis shows that the $CSCR_s$ derived from the small-signal stability analysis and the $CSCR_v$ derived from the voltage stability analysis are different from each other. Moreover, which one of the two is bigger is not necessarily the same from case to case. As a result, the study is divided into two perspectives.

A. Reduction of the $CSCR_v$

As aforementioned, the highest possible $CSCR_v$ of a charging system is two, assuming the charger's PF is unity and the GIR of the grid is infinite. The $CSCR_v$ can be reduced, as indicated by (17), by increasing the charger's reactive power injection. However, with a fixed apparent power capacity, increasing the reactive power injection inevitably decreases the maximum charging power. A smaller charging power results in a longer charging time, which negatively affects consumers' experience. Thus, for a normal charger without reactive power injection ability, the worst case $CSCR_v$ is fixed at 2. Obviously, the flexibility of reducing the $CSCR_v$

is limited because it is constrained by the fundamental maximum power transfer theorem.

B. Reduction of the $CSCR_s$

Compared with reducing $CSCR_v$, decreasing the $CSCR_s$ has more flexibility because the $CSCR_s$ is influenced by the control of the charger's rectifier. Methods to reduce the $CSCR_s$ by modifying a charger's rectifier control will be elaborated on based on the example given by Table I. As seen in Fig. 6, for a charger's rectifier, $Z_{dd}(s)$ has the dominant influence on the charging system's stability, because $Z_{qq}(s)$ does not have non-passive region. Therefore, the discussion focuses on the influence of the control on $Z_{dd}(s)$.
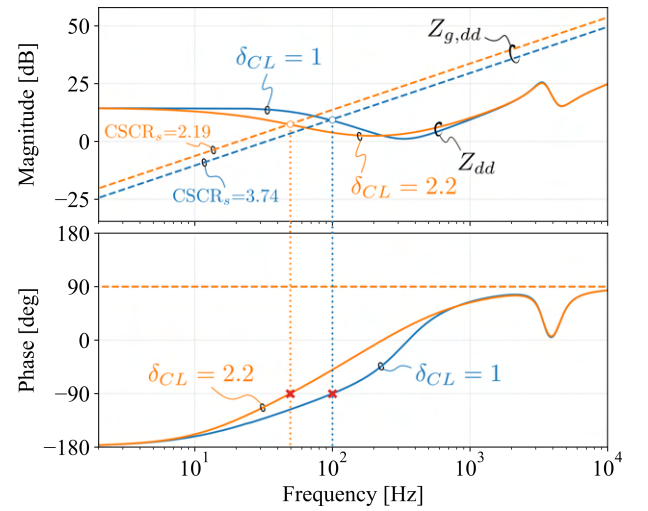

Fig. 8. Influence of the CL damping ratio δ_{CL} on the $Z_{dd}(s)$ and the $CSCR_s$

Fig. 8 illustrates the influence of the rectifier's CL damping ratio δ_{CL} on the $Z_{dd}(s)$. With a higher δ_{CL}, the non-passive frequency range of the $Z_{dd}(s)$ is narrower. Consequently, the $CSCR_s$ decrease from 3.74 to 2.12. Note that the CSCR of the charging system equals the $CSCR_s$ since the $CSCR_s$ in both cases is higher than 2, which is the value of the $CSCR_v$. Thus, the CSCR of the charging system is also reduced to 2.12 by increasing the δ_{CL}., which is verified by the simulation results depicted in Fig. 9. The SCR in the simulation is fixed at 2.5. Before $t_0 = 2.5$ s, the δ_{CL} equals 2.2 and the charging system is stable. After t_0, the δ_{CL} is decreased to 1. As a result, the CSCR is increased from 2.19 to 3.74, which is illustrated in Fig. 8. Therefore, the charging system loses stability after decreasing the δ_{CL}, because the SCR is smaller than the new CSCR.

Another effective method to reduce the $CSCR_s$ of a charging system is decreasing the rectifier's VL cutoff
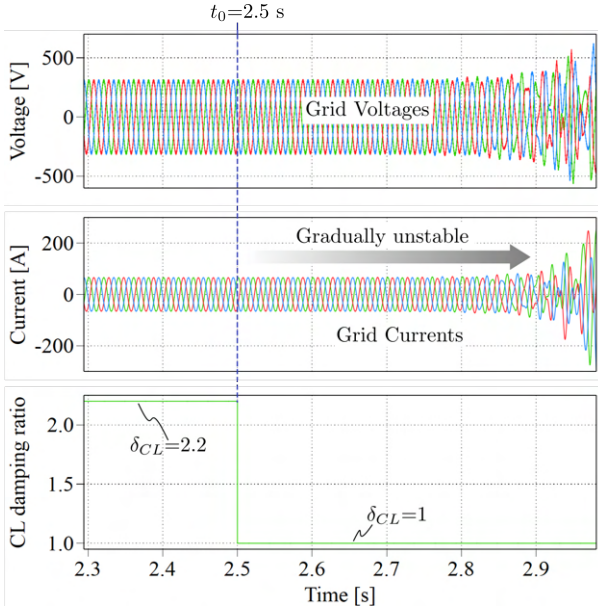
Fig. 9. Simulation of the influence of the CL damping ratio δ_{CL} on the stability of the charging system.
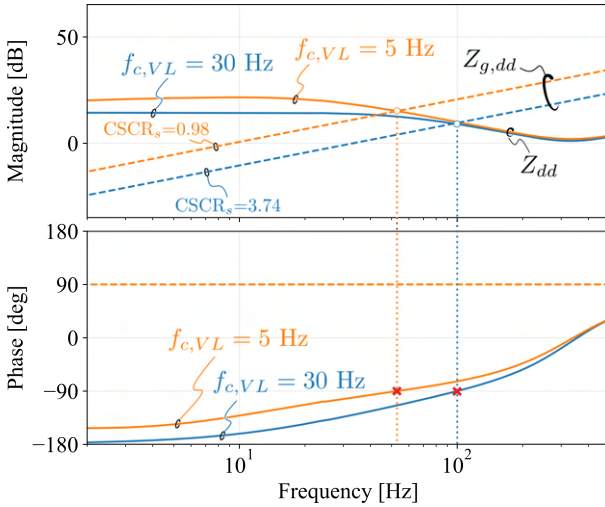

Fig. 10. Influence of the VL cutoff frequency $f_{c,VL}$ on the $Z_{dd}(s)$ and the $CSCR_s$.

frequency $f_{c,VL}$, which is shown in Fig. 10. As seen, the charger's $Z_{dd}(s)$ has the non-passive characteristic until a lower frequency with a decreased $f_{c,VL}$. As a result, the $CSCR_s$ is reduced to 0.98. However, in this case, the $CSCR_s$ is smaller than the $CSCR_v$. Therefore, the CSCR of the charging system is determined by the $CSCR_v$, which is 2.

Fig. 11 shows the simulation results evincing that reducing the $f_{c,VL}$ of a charger's rectifier can reduce the CSCR of a charging system. The CSCR of the charging system specified by Table I is 3.74. In the simulation,

the SCR of the system before t_0 is 3. The $f_{c,VL}$ is reduced from 30 Hz to 5 Hz, leading to a reduced CSCR to stabilize the charging system in this weak grid condition. After t_0, the SCR gradually decreases until 2. The system is still stable in this case. Nevertheless, at t_1 the SCR further decreases to 1.9 leading to instability. The simulation results prove that reducing the rectifier's $f_{c,VL}$ can decrease the CSCR. However, the CSCR of the system cannot be decreased to below 2 by modifying the rectifier's control because of the constraint of the $CSCR_v$.
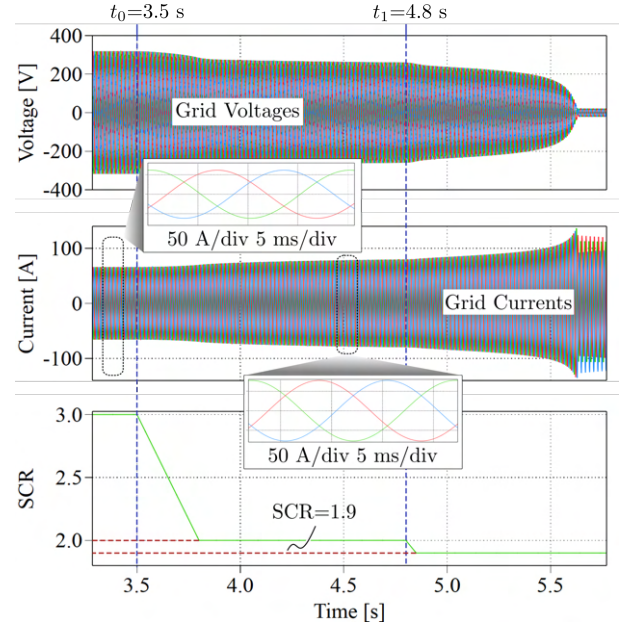

Fig. 11. The charging system can operate stably when SCR=2 after reducing the VL cutoff frequency $f_{c,VL}$, which indicates the CSCR is reduced from 3.74 to 2. However, the CSCR cannot be reduced to below 2 by modifying the control because of the constraint of the $CSCR_v$.

V. CONCLUSION

This paper has compared the two commonly used definitions of the CSCR of a grid-converter system and clarified the differences between them. Specifically, the $CSCR_v$ is defined from the voltage stability perspective and the $CSCR_s$ is defined from the small-signal stability perspective. The bigger one between the two determines the CSCR of the grid-converter system. Further, the simplified methods for calculating the $CSCR_v$ and the $CSCR_s$ of an EV charging system are proposed. Based on the calculated $CSCR_v$ and $CSCR_s$, the CSCR of the charging system can be easily obtained. Simulations are carried out to validate the calculated $CSCR_v$ and $CSCR_s$. Finally, the design suggestions for an EV charger to

reduce the CSCR$_v$ and the CSCR$_s$ are studied. Adopting the design suggestions can improve an EV charging system's robustness against the grid strength weakening, which is verified with simulations.

REFERENCES

[1] A. Ahmad, Z. Qin, T. Wijekoon, and P. Bauer, "An overview on medium voltage grid integration of ultra-fast charging stations: Current status and future trends," *IEEE Open Journal of the Industrial Electronics Society*, vol. 3, pp. 420–447, 2022.

[2] L. Wang, Z. Qin, L. B. Larumbe, and P. Bauer, "Python supervised co-simulation for a day-long harmonic evaluation of ev charging," *Chinese J. Elect. Eng.*, vol. 7, no. 4, pp. 15–24, 2021.

[3] J. Sun, "Impedance-based stability criterion for grid-connected inverters," *IEEE Trans. Power Electron.*, vol. 26, no. 11, pp. 3075–3078, 2011.

[4] *IEEE Guide for Planning DC Links Terminating at AC Locations Having Low Short-Circuit Capacities*, IEEE Std. 1204, 1997.

[5] L. B. Larumbe, Z. Qin, L. Wang, and P. Bauer, "Impedance modeling for three-phase inverters with double synchronous reference frame current controller in the presence of imbalance," *IEEE Trans. Power Electron.*, vol. 37, no. 2, pp. 1461–1475, 2022.

[6] L. Beloqui Larumbe, Z. Qin, and P. Bauer, "Guidelines for stability analysis of the DDSRF-PLL using LTI and LTP modelling in the presence of imbalance," *IEEE Open J. Ind. Electron. Soc.*, pp. 1–1, 2022.

[7] J. Lei, Z. Qin, W. Li, P. Bauer, and X. He, "Stability region exploring of shunt active power filters based on output admittance modeling," *IEEE Trans. Ind. Electron.*, vol. 68, no. 12, pp. 11 696–11 706, 2021.

[8] P. Kundur, *Power System Stability and Control*. New York: McGraw-Hill, 1994.

[9] M. Belkhayat, "Stability criteria for ac power systems with regulated loads," Ph.D. dissertation, 1997.

[10] B. Wen, D. Boroyevich, R. Burgos, P. Mattavelli, and Z. Shen, "Analysis of d-q small-signal impedance of grid-tied inverters," *IEEE Trans. Power Electron.*, vol. 31, no. 1, pp. 675–687, 2016.

[11] W. Dong, H. Xin, D. Wu, and L. Huang, "Small signal stability analysis of multi-infeed power electronic systems based on grid strength assessment," *IEEE Trans. Power Syst.*, vol. 34, no. 2, pp. 1393–1403, 2019.

[12] Z. Qin, L. Wang, and P. Bauer, "Review on power quality issues in ev charging," in *2022 IEEE 20th International Power Electronics and Motion Control Conference (PEMC)*, pp. 360–366, 2022.

[13] L. Wang, Z. Qin, and P. Bauer, "A gradient-descent optimization assisted gray-box impedance modeling of ev chargers," *IEEE Trans. Power Electron.*, vol. 38, no. 7, pp. 8866–8879, 2023.

[14] J. Xiao, L. Wang, Z. Qin, and P. Bauer, "A resilience enhanced secondary control for ac micro-grids," *IEEE Trans. Smart Grid*, pp. 1–1, 2023 (early access).

[15] L. Wang, Z. Qin, T. Slangen, P. Bauer, and T. van Wijk, "Grid impact of electric vehicle fast charging stations: Trends, standards, issues and mitigation measures - an overview," *IEEE Open J. Power Electron.*, vol. 2, pp. 56–74, 2021.

[16] J. Xu, T. B. Soeiro, Y. Wang, F. Gao, H. Tang, and P. Bauer, "A hybrid modulation featuring two-phase clamped discontinuous PWM and zero voltage switching for 99% efficient dc-type ev charger," *IEEE Trans. Veh. Technol.*, vol. 71, no. 2, pp. 1454–1465, 2022.

[17] B. Wen, R. Burgos, D. Boroyevich, P. Mattavelli, and Z. Shen, "Ac stability analysis and dq frame impedance specifications in power-electronics-based distributed power systems," *IEEE J. Emerg. Sel. Topics Power Electron.*, vol. 5, no. 4, pp. 1455–1465, 2017.

[18] R. Burgos, D. Boroyevich, F. Wang, K. Karimi, and G. Francis, "On the ac stability of high power factor three-phase rectifiers," in *2010 IEEE Energy Conversion Congress and Exposition*, pp. 2047–2054, 2010.

[19] *IEEE Standard for Interconnection and Interoperability of Distributed Energy Resources with Associated Electric Power Systems Interfaces*, IEEE Std. 1547, 2018.